Large magnetic refrigerant capacity in Gd$_{71}$Fe$_3$Al$_{26}$ and Gd$_{65}$Fe$_{20}$Al$_{15}$ amorphous alloys

Q. Y. Dong, B. G. Shen,[a)] J. Chen, J. Shen, F. Wang, H. W. Zhang, and J. R. Sun
State Key Laboratory for Magnetism, Institute of Physics, Chinese Academy of Sciences, Beijing 100190, People's Republic of China

Magnetic entropy change and refrigerant capacity of Gd-based amorphous Gd$_{71}$Fe$_3$Al$_{26}$ and Gd$_{65}$Fe$_{20}$Al$_{15}$ alloys are investigated. The refrigerant capacities reach 750 and 726 J kg^{-1} for Gd$_{71}$Fe$_3$Al$_{26}$ and Gd$_{65}$Fe$_{20}$Al$_{15}$, respectively, which are much larger than those of all magnetocaloric materials ever reported. The peak values of magnetic entropy change under a field change of 0–5 T are 7.4 J kg^{-1} K^{-1} at 117.5 K and 5.8 J kg^{-1} K^{-1} at 182.5 K for Gd$_{71}$Fe$_3$Al$_{26}$ and Gd$_{65}$Fe$_{20}$Al$_{15}$, respectively. A very large refrigerant capacity and a considerable magnetic entropy change jointly make them attractive candidates for magnetic refrigerant. © *2009 American Institute of Physics.* [DOI: 10.1063/1.3072631]

I. INTRODUCTION

Magnetic refrigeration based on the magnetocaloric effect (MCE) has attracted much attention due to its potential advantages such as environmental friendliness and relatively high efficiency over traditional vapor-compression refrigeration.[1] Currently, a large isothermal magnetic entropy change (ΔS_M), as an important parameter for evaluating the amount of the MCE, has been found in materials with a first-order phase transition such as Gd$_5$(Si,Ge)$_4$,[2] La(Fe,Si)$_{13}$,[3,4] MnAs,[5,6] MnFe(P,As),[7] Ni$_2$MnGa,[8] etc. The first-order phase transition yields an intense and sharp magnetocaloric response peak while the second-order phase transition produces a broader and less intense peak. However, the refrigerant capacity (RC), that is, the amount of heat that can be transferred in one thermodynamic cycle,[1,9] which also takes into account the width and shape of ΔS_M versus T curve, is a more relevant parameter when evaluating the technological interest in a refrigerant material. Furthermore, the hysteresis loss as well as the slow kinetics inherent in materials with a first-order phase transition may reduce the actual magnetocaloric efficiency of these materials. Thus, a compromise between the peak entropy change and the width of the peak is necessary for a working prototype, as discussed by Wood and Potter.[9]

Recently, soft magnetic amorphous alloys with a second-order phase transition have become attractive for magnetic refrigerant applications due to their reduced magnetic hysteresis (actually negligible), high electrical resistivity (which would decrease eddy current loss), high corrosion resistance, and tunable Curie temperature (T_C).[10–14] Among them, the special attention should be paid to the heavy rare earth based amorphous alloys for they possess large magnetic moments and profuse magnetic structures. In this work, the magnetic properties and MCEs of two Gd-based amorphous alloys,

Gd$_{71}$Fe$_3$Al$_{26}$ and Gd$_{65}$Fe$_{20}$Al$_{15}$, are reported. To our knowledge, of all the reported magnetocaloric materials, the present samples own the largest RC.

II. EXPERIMENTS

The Gd$_{71}$Fe$_3$Al$_{26}$ and Gd$_{65}$Fe$_{20}$Al$_{15}$ ingots were prepared by arc melting high-purity elemental constituents in an argon atmosphere and then they were melt spun into ribbons by single roller melt spinning at a surface speed of 50 m/s (i.e., the quenching ratio is about 10^6 K/s). The melting temperature for Gd$_{71}$Fe$_3$Al$_{26}$ or Gd$_{65}$Fe$_{20}$Al$_{15}$ ingot is between 1273 and 1373 K. The amorphous character of the as-quenched alloys was confirmed by x-ray diffraction. The measurement of magnetization as a function of temperature and field was carried out by using a Quantum Design superconducting quantum interference device magnetometer. The heat capacity measurements were performed using physical property measurement system (Quantum Design).

The magnetic entropy change due to the application of a magnetic field H was evaluated by treating the temperature and field dependent magnetization curves with the numerical approximation to the equation

$$\Delta S_M = \int_0^H \left(\frac{\partial M}{\partial T} \right)_H dH, \tag{1}$$

where the partial derivative is replaced by a finite difference and the integration is performed numerically.

III. RESULTS AND DISCUSSION

Figure 1 shows the x-ray diffraction patterns for the as-spun Gd$_{71}$Fe$_3$Al$_{26}$ and Gd$_{65}$Fe$_{20}$Al$_{15}$ ribbons, where there appear broad diffraction peaks but no appreciable peaks corresponding to a crystalline phase, indicating that each alloy has an amorphous structure.

Figure 2(a) illustrates the temperature dependences of magnetization $M(T)$ for Gd$_{71}$Fe$_3$Al$_{26}$ and Gd$_{65}$Fe$_{20}$Al$_{15}$ alloys in fields of 0.01 and 0.1 T under the zero-field cooling (ZFC) and field cooling (FC) conditions. The ZFC branch

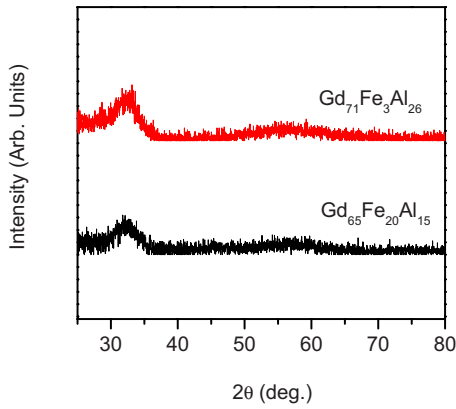a)Author to whom correspondence should be addressed. Electronic mail: shenbg@g203.iphy.ac.cn.

FIG. 1. (Color online) X-ray diffraction patterns of the amorphous $Gd_{71}Fe_3Al_{26}$ and $Gd_{65}Fe_{20}Al_{15}$ ribbons at room temperature.

was measured on heating under a measuring field after initially cooling from 250 to 5 K under a zero field while the FC branch was measured on cooling from 250 to 5 K under the same measuring field. The irreversibility between the ZFC and the FC branches at low temperature can be seen for $Gd_{71}Fe_3Al_{26}$ alloy under a field of 0.01 T. However, the irreversibility behavior can be easily dissolved even under a low field of 0.1 T. Different from $Gd_{71}Fe_3Al_{26}$ alloy, $Gd_{65}Fe_{20}Al_{15}$ alloy just shows a very weak spin freezing be-
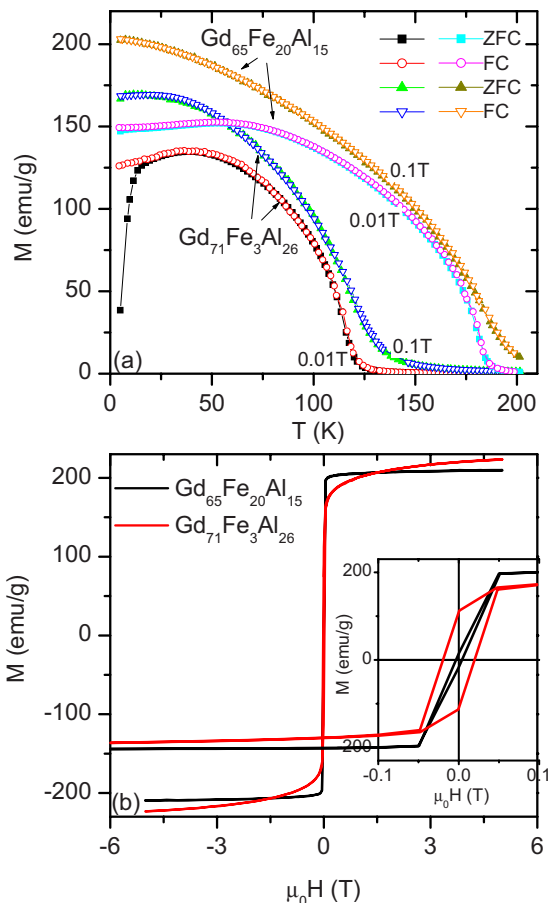

FIG. 2. (Color online) Temperature dependences of magnetization under fields of (a) 0.01 and 0.1 T and magnetic hysteresis loops at (b) 5 K for $Gd_{71}Fe_3Al_{26}$ and $Gd_{65}Fe_{20}Al_{15}$ alloys. The inset of (b) shows the enlarged part of magnetic hysteresis loops.
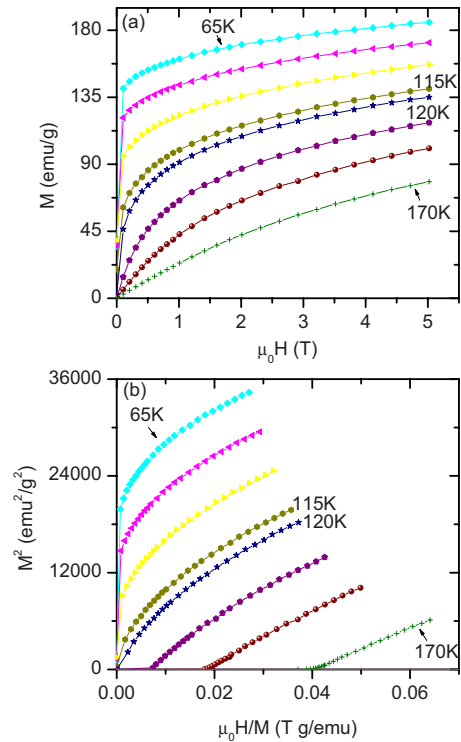

FIG. 3. (Color online) Isothermal magnetization as a function of (a) magnetic field and (b) Arrott plots for $Gd_{71}Fe_3Al_{26}$ alloy in a temperature range of 65–170 K.

havior under a field of 0.01 T. The ZFC and the FC branches become identical to each other under a field of 0.1 T. At high temperatures, a ferromagnetic-to-paramagnetic phase transition is found in each alloy. The values of T_C, determined as the temperature corresponding to the minimum in dM/dT under a field of 0.01 T, are 114 K for $Gd_{71}Fe_3Al_{26}$ and 180 K for $Gd_{65}Fe_{20}Al_{15}$, respectively. Scarcely any thermal hysteresis can be observed in the vicinity of T_C. Figure 2(b) displays the magnetic hysteresis loops of $Gd_{71}Fe_3Al_{26}$ and $Gd_{65}Fe_{20}Al_{15}$ at 5 K. The saturated magnetization for $Gd_{71}Fe_3Al_{26}$ reaches 4.6 μ_B/f.u., which is slightly larger than that of $Gd_{65}Fe_{20}Al_{15}$ (4.4 μ_B/f.u.). Nevertheless, $Gd_{65}Fe_{20}Al_{15}$ is easier to be magnetized and demagnetized and has a smaller coercivity (~40 Oe) than $Gd_{71}Fe_3Al_{26}$ (~190 Oe) [see the inset of Fig. 2(b)].

The MCEs of Gd-based amorphous alloys were obtained by using Eq. (1) through the isothermal magnetization curves at different temperatures. As an example, Fig. 3(a) displays the isothermal magnetization as a function of magnetic field in a temperature range of 65–170 K for amorphous $Gd_{71}Fe_3Al_{26}$ alloy. The sweeping rate of field was slow enough to ensure that the data are recorded in an isothermal process. Figure 3(b) shows the corresponding Arrott plot[15] for $Gd_{71}Fe_3Al_{26}$ alloy, from which no inflection or negative slope is observed as an indication of metamagnetic transition above T_C, indicating a nature of the second-order phase transition.

Figure 4 shows $-\Delta S_M$ as a function of temperature for $Gd_{71}Fe_3Al_{26}$ and $Gd_{65}Fe_{20}Al_{15}$ alloys under field changes of 0–2 and 0–5 T. The peak values of $-\Delta S_M$ under a field change of 0–5 T are 7.4 J kg^{-1} K^{-1} at 117.5 K and

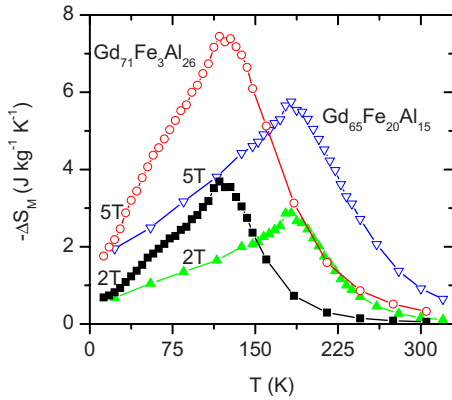FIG. 4. (Color online) Magnetic entropy changes as a function of temperature for $Gd_{71}Fe_3Al_{26}$ and $Gd_{65}Fe_{20}Al_{15}$ alloys under field changes of 0–2 and 0–5 T.

FIG. 5. (Color online) Temperature dependence of the adiabatic temperature change for $Gd_{71}Fe_3Al_{26}$ alloy under field changes of 0–2 and 0–5 T. The inset shows the zero-field heat capacity of $Gd_{71}Fe_3Al_{26}$

5.8 J kg^{-1} K^{-1} at 182.5 K for $Gd_{71}Fe_3Al_{26}$ and $Gd_{65}Fe_{20}Al_{15}$, respectively. Although $-\Delta S_M$ values are slightly lower than those of Gd and some amorphous alloys reported recently,[13,16–18] the temperature ranges of half maximum of the entropy change peak reach 131 K for $Gd_{71}Fe_3Al_{26}$ and 169 K for $Gd_{65}Fe_{20}Al_{15}$ under a field change of 0–5 T. A large temperature width of the $-\Delta S_M$ peak (when the peak value is identical) is advantageous to obtain a large RC characterizing the refrigerant efficiency of the materials. The RC was measured in literature by using different methods.[9,19] Here the RC values are determined by numerically integrating the area under the $-\Delta S_M$-T curve, with the temperature at half maximum of the peak used as the integration limit.[19] By using this method the RC values for $Gd_{71}Fe_3Al_{26}$ and $Gd_{65}Fe_{20}Al_{15}$ under a field change of 0–5 T are obtained to be 750 and 726 J kg^{-1}, respectively. These values are much larger than those of most classical crystalline magnetic refrigeration materials such as Gd (556 J kg^{-1}) (Ref. [20]) and $Gd_5Si_2Ge_2$ (305 J kg^{-1}).[21] They are also much larger than that of amorphous $Gd_{55}Ni_{25}Al_{20}$ alloy (640 J kg^{-1}), which has the largest RC value among the magnetocaloric materials reported.[16] The high RC is due to the glassy structure that extends the large MCE into a larger temperature range. For comparison, magnetocaloric properties of some typical materials as well as our materials under the same field change are listed in Table I.
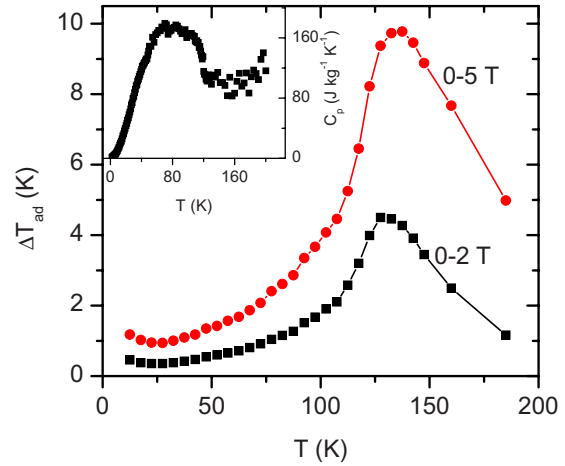
Figure 5 shows the temperature dependence of MCE in terms of adiabatic temperature change (ΔT_{ad}) for $Gd_{71}Fe_3Al_{26}$, calculated from the magnetic entropy change and the temperature variation in zero-field heat-capacity data (see the inset of Fig. 5). The maximum values of ΔT_{ad} are found to be 4.5 and 9.8 K for field changes of 0–2 and 0–5 T, respectively. These values are much larger than those in $Gd_{0.7}Ni_{0.3}$ amorphous alloy (3.3 K for 0–8 T).[23]

IV. CONCLUSION

Amorphous $Gd_{71}Fe_3Al_{26}$ and $Gd_{65}Fe_{20}Al_{15}$ alloy ribbons show spin freezing behavior at low temperatures under a very small field. However, this irreversibility behavior can be dissolved even under a small field of 0.1 T. The peak values of $-\Delta S_M$ under a field change of 0–5 T are 7.4 J kg^{-1} K^{-1} at 117.5 K and 5.8 J kg^{-1} K^{-1} at 182.5 K for $Gd_{71}Fe_3Al_{26}$ and $Gd_{65}Fe_{20}Al_{15}$, respectively. The values of RC reach 750 and 726 J kg^{-1} for $Gd_{71}Fe_3Al_{26}$ and $Gd_{65}Fe_{20}Al_{15}$, respectively, which are much larger than that of amorphous $Gd_{55}Ni_{25}Al_{20}$ alloy (640 J kg^{-1}) that has the largest RC value among the magnetocaloric materials reported.

TABLE I. Magnetocaloric properties of some typical magnetic refrigerants including amorphous and crystalline materials. A and C stand for amorphous and crystalline alloys, respectively.

Material	Structure	Transition temperature (K)	$-\Delta S_M^{max}$ (0–5 T) (J kg^{-1} K^{-1})	RC (0–5 T) (J kg^{-1})	Reference
$Gd_{71}Fe_3Al_{26}$	A	117.5	7.4	750	This work
$Gd_{65}Fe_{20}Al_{15}$	A	182.5	5.8	726	This work
Gd	C	293	9.8	556	20
$Gd_5Si_2Ge_2$	C	276	18.6	305	21
$Gd_{55}Co_{20}Al_{25}$	A	103	8.8	514	16
$Gd_{55}Ni_{25}Al_{20}$	A	78	8.0	640	16
$Gd_{33}Er_{22}Al_{25}Co_{20}$	A	52	9.5	574	17
$Gd_{53}Al_{24}Co_{20}Zr_3$	A	93	9.4	590	17
$Dy_{50}Gd_7Al_{23}Co_{20}$	A	26	9.77	290	13
$Gd_{36}Y_{20}Al_{24}Co_{20}$	A	53	7.76	459	22

ACKNOWLEDGMENTS

[1] K. A. Gschneidner, Jr., V. K. Pecharsky, and A. O. Tsokol, Rep. Prog. Phys. **68**, 1479 (2005).

[2] V. K. Pecharsky and K. A. Gschneidner, Jr., Phys. Rev. Lett. **78**, 4494 (1997).

[3] F. X. Hu, B. G. Shen, J. R. Sun, and X. X. Zhang, Chin. Phys. **9**, 550 (2000).

[4] F. X. Hu, B. G. Shen, J. R. Sun, Z. H. Cheng, G. H. Rao, and X. X. Zhang, Appl. Phys. Lett. **78**, 3675 (2001).

[5] H. Wada and Y. Tanabe, Appl. Phys. Lett. **79**, 3302 (2001).

[6] S. Gama, A. A. Coelho, A. de Campos, A. M. Carvalho, F. C. G. Gandra, P. J. von Ranke, and N. A. de Oliveira, Phys. Rev. Lett. **93**, 237202 (2004).

[7] O. Tegus, E. Bruck, K. H. J. Buschow, and F. R. de Boer, Nature (London) **415**, 150 (2002).

[8] F. X. Hu, B. G. Shen, and J. R. Sun, Appl. Phys. Lett. **76**, 3460 (2000).

[9] M. E. Wood and W. H. Potter, Cryogenics **25**, 667 (1985).

[10] P. Didukh and A. Slawska-Waniewska, J. Magn. Magn. Mater. **254–255**, 407 (2003).

[11] S. Atalay, H. Gencer, and V. S. Kolat, J. Non-Cryst. Solids **351**, 2373 (2005).

[12] V. Franco, J. S. Blázquez, C. F. Conde, and A. Vonde, Appl. Phys. Lett. **88**, 042505 (2006).

[13] Q. Luo, D. Q. Zhao, M. X. Pan, and W. H. Wang, Appl. Phys. Lett. **90**, 211903 (2007).

[14] D. Chen, A. Takeuchi, and A. Inoue, J. Alloys Compd. **440**, 199 (2007).

[15] A. Arrott, Phys. Rev. **108**, 1394 (1957).

[16] J. Du, Q. Zheng, Y. B. Li, Q. Zhang, D. Li, and Z. D. Zhang, J. Appl. Phys. **103**, 023918 (2008).

[17] Q. Luo, D. Q. Zhao, M. X. Pan, and W. H. Wang, Appl. Phys. Lett. **89**, 081914 (2006).

[18] H. Fu, X. Y. Zhang, H. J. Yu, B. H. Teng, and X. T. Zu, Solid State Commun. **145**, 15 (2008).

[19] K. A. Gschneidner, Jr., V. K. Pecharsky, A. O. Pecharsky, and C. B. Zimm, Mater. Sci. Forum **315–317**, 69 (1999).

[20] Y. X. Li, F. X. Hu, J. R. Sun, and B. G. Shen, J. Phys. D: Appl. Phys. **41**, 245005 (2008).

[21] V. Provenzano, A. J. Shapiro, and R. D. Shull, Nature (London) **429**, 853 (2004).

[22] L. Liang, X. Hui, Y. Wu, and G. L. Chen, J. Alloys Compd. **457**, 541 (2008).

[23] X. Y. Liu, J. A. Barclay, R. B. Gopal, M. Foldeaki, R. Chahine, T. K. Bose, P. J. Schuler, and J. L. Lacombe, J. Appl. Phys. **79**, 1630 (1996).